VICTORIA UNIVERSITY
MELBOURNE AUSTRALIA

Predicting the influence of operating conditions on DCMD flux and thermal efficiency for incompressible and compressible membrane systems

Predicting the influence of operating conditions on DCMD flux and thermal efficiency for incompressible and compressible membrane systems

Jianhua Zhang[a], Stephen Gray[a], Jun-De Li[a, b*]

[a]*Institute of Sustainability and Innovation, Victoria University, PO Box 14428, Melbourne, Victoria 8001, Australia*

[b]*School of Engineering and Science, Victoria University, PO Box 14428, Melbourne, Victoria 8001, Australia*

Corresponding author, Tel.: +61-3-9919 4105, E-mail: jun-de.li@vu.edu.au

Abstract

Membrane distillation (MD) is a hybrid of thermal distillation and membrane separation. As a thermal distillation process, MD is an energy intensive technique. Therefore, it is important to select optimum operation parameters to maximise both the flux and energy efficiency, even though low grade or waste heat maybe employed in the process. In this paper, a model originally developed for Direct Contact Membrane Distillation (DCMD) using a compressible membrane is employed to predict the thermal efficiency and flux for both compressible and incompressible membrane systems. The predicted thermal efficiency was also compared with experimental results, and the errors were mostly within the range of experimental variation (±5%). As a result of membrane compressibility, the thermal conductivity and vapour permeability of the membrane were altered, causing a change in flux and energy efficiency. If a compressible membrane is used, it was found from the predicted results, that increasing stream velocity will reduce the thermal efficiency and even reduce flux once the increased pressure associated with the higher flows is in the range to compress the membrane. Increasing temperature either on feed side or on permeate side will increase thermal efficiency. In scaling up the process using a compressible membrane, it is necessary to reduce the pressure drop across the module in the DCMD process to maximise energy efficiency and flux. Since the operating temperature is normally not adjustable when low grade waste heat is employed, optimising the flowrates and pressure drops are the key factors for optimising flux and thermal efficiency.

1. Introduction

Membrane distillation (MD) is a hybrid of thermal distillation and membrane separation [1]. The concept of MD was first described in technical literature in 1967 [2]. Numerous researchers around the world have contributed to the understanding of the process [3, 4].

MD has 100% theoretical rejection of non-volatile components and can utilise low grade heat sources of 40-80°C. The path length of the vapour phase in MD is approximately the membrane thickness (~100 μm), which is much shorter than that for the Multiple Stage Flash (MSF) distillation process and other thermal desalination processes. MD can also be used to treat high concentration or supersaturated solutions, because its driving force is not as sensitive to concentration as is the case for reverse osmosis (RO). Therefore, it could be an effective method to reduce the volume of waste discharges or even convert a reject stream to a high value concentrated liquid. It also is a potential commercial desalination technique if it can be combined with solar energy, geothermal energy or waste heat available in power stations or chemical plants. However, as a thermal distillation process, MD is also an energy intensive technique. Hence, if low cost thermal energy is not available or in low supply, efficient utilisation of energy is required for effective production of fresh water.

Even though the DCMD process was developed in the late 1960s, it was not commercially adopted at that time, partly because membranes with characteristics suitable for MD were not available. Furthermore, the slow progress in development was also caused by negative opinions about the economics of the process [5], which were performed using non-optimal

membranes and systems. For instance, using typical data, the temperature polarization coefficient (TPC) of DCMD defined in Eq. (1) by Schofield et al. [6] for their system was estimated to be 0.32. This means that when the temperature difference between the bulk flows of the hot and cold streams was 10°C, the actual temperature difference across the membrane was only 3.2°C.

$$TPC = \frac{T_1 - T_2}{T_f - T_p} \tag{1}$$

where T_1 and T_2 are the interface temperatures on feed and permeate sides, and T_f and T_p are the bulk temperatures on the feed and permeate sides.

Since the 1980s, with the availability of new membranes, more research has been focused on membrane distillation and many novel MD modules were designed based on improved understanding of the mass and heat transfer principles of MD [7-9]. Recently, the membrane fabrication research has achieved continuous breakthroughs due to the efforts of various research groups and the development of new technologies [10-13].

In DCMD, the pressure applied on the membrane surface is mainly determined by either the hydrodynamic conditions which are directly related to the flowrate, or by backpressure applied to the system. In this work, the increase in pressure associated with high flowrates is considered. At high flowrates, high turbulence will increase the heat transfer so as to increase the interface temperature and permeate flux, but the high turbulence will also incur a higher compressive pressure on the membrane surface. For a compressible membrane, the increased compressive pressure will reduce the advantages of enhanced heat transfer in the feed and permeate streams due to high velocity, and may even result in a lower flux at higher velocity. Therefore, it is necessary to assess the energy efficiency and flux of compressible membranes at different velocities by correlating the increased velocity with escalated pressure drop in the module.

In paper [14], the modelling focused on predicting the influence of pressure on flux and thermal efficiency individually. In this paper, the thermal efficiency and flux of the compressible membrane was modelled by combining stream flowrate with the resulted hydraulic pressure, and the influence of varying velocity on a single side of the membrane on the thermal efficiency and flux of incompressible membrane was also predicted. To the authors' knowledge, there are few modelling papers that discuss the relationship between thermal efficiency and process parameters in DCMD process. A published paper [15] did some theoretical works on these aspects, in which optimum parameters were predicted for operating DCMD. However, they did not consider membrane compressibility and the findings from our work predicted different outcomes. The efficiency of the DCMD process in this paper is analysed using thermal efficiency [16]. The relationship between the pressure and stream velocity was measured experimentally. The accuracy of the model predictions for thermal efficiency was also assessed experimentally under different conditions before it was employed for further predictions.
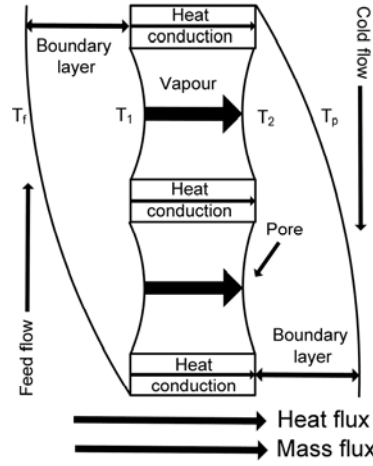
2. Theory and mathematical modelling

Fig.1 Heat and mass transfer through a DCMD membrane

In DCMD, the driving force for mass transfer is the vapour pressure difference that arises from the temperature difference between the liquid phases on both sides of the membrane. Thus, DCMD performance relies on the complex relationships between simultaneous heat and mass transfers, which are in the same direction from the feed side to the permeate side. Figure 1 shows the schematic of DCMD heat and mass transfer. Assuming no heat loss through module walls to the ambient environment, the total heat flux can be expressed as [3, 11]:

$$Q \approx \alpha_f(T_f - T_1)Wdx = \left(\frac{\lambda}{b}(T_1 - T_2) + Jh_{latent}\right)Wdx \approx \alpha_P(T_2 - T_p)Wdx$$

in which $\lambda = (1 - \varepsilon)\lambda_{solid} + \varepsilon\lambda_{air}$ \hfill (2)

where Q is the overall heat transfer, α_f and α_p are the heat transfer coefficients on the hot side and cold side respectively, W is the membrane width, λ is the thermal conductivity of the membrane, b is membrane thickness, J is the vapour flux through the membrane, T_1 and T_2 are interface temperatures of the feed and permeate respectively, T_f and T_p are the bulk temperatures of on the feed and permeate sides, λ_{solid} and λ_{air} are respectively the thermal conductivities of the active layer material and air. In Eq. (2), $\lambda(T_1-T_2)/b$ is the sensible heat transfer across the membrane and Jh_{latent} is the latent heat transfer. Therefore, the thermal efficiency (expressed as a percentage) can be defined as [16]:

$$E = \frac{Jh_{latent}}{Q} \times 100\%$$ \hfill (3)

The assumptions for the mathematical model, details of programming and equations for correlating the hydraulic pressure with the membrane compressibility were presented in Zhang et. al [14]. Theoretically, the feed concentration should have influence on the permeate flux, and 5% flux variation incurred by the feed concentration was reported [12]. However, there was no detectable flux variation observed in these experiments as the feed changed from deionised water to 1-2 wt% NaCl solution possibly due to the spacer (turbulence promoter) which substantially diminished the concentration boundary layer. Therefore, in our modelling study the influence of feed concentration is ignored. The flow chart for calculating the temperature development in both the feed and permeate streams is shown in Fig. 2.
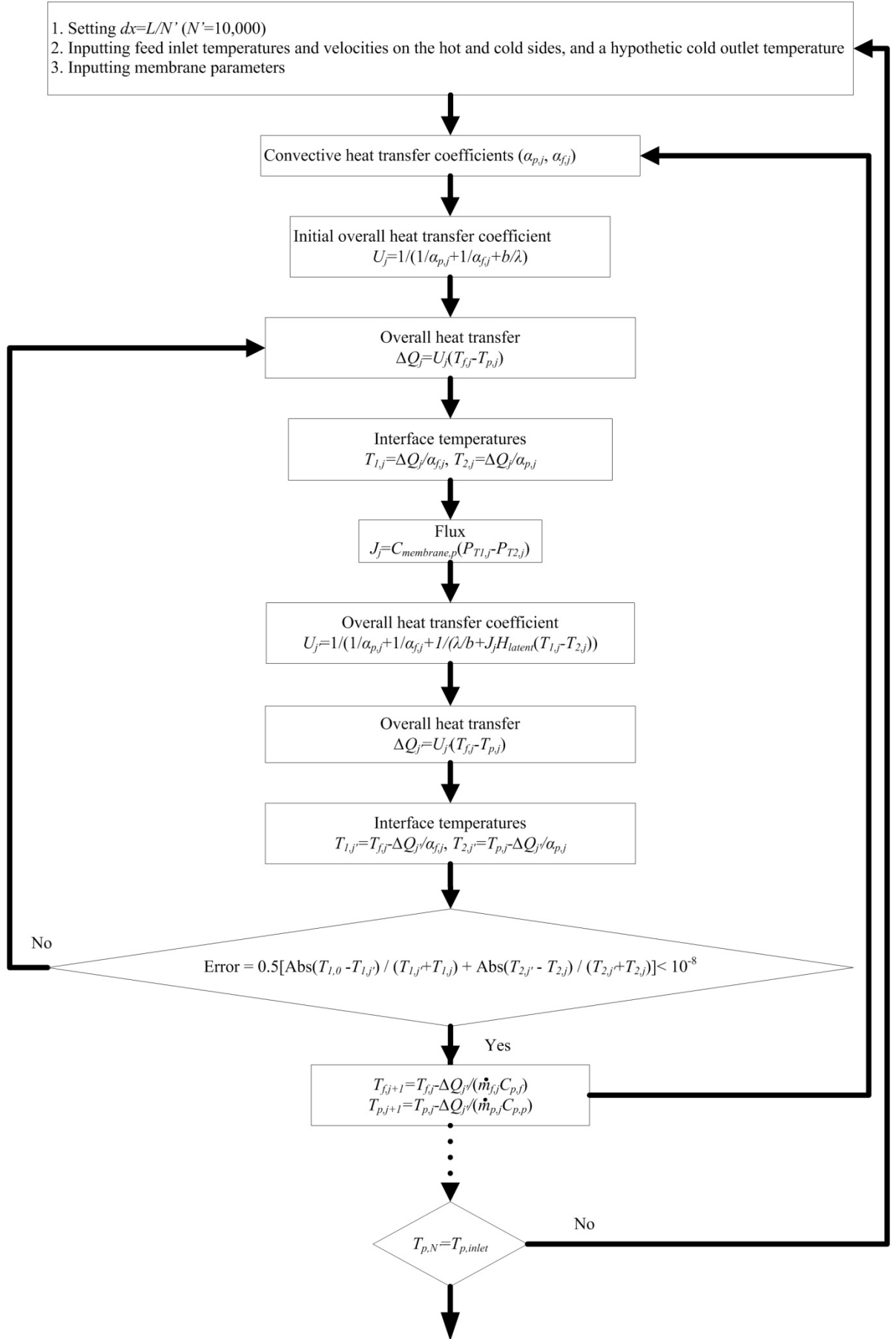
1. Setting $dx=L/N'$ (N'=10,000)
2. Inputting feed inlet temperatures and velocities on the hot and cold sides, and a hypothetic cold outlet temperature
3. Inputting membrane parameters

Convective heat transfer coefficients ($\alpha_{p,j}$, $\alpha_{f,j}$)

Initial overall heat transfer coefficient
$U_j=1/(1/\alpha_{p,j}+1/\alpha_{f,j}+b/\lambda)$

Overall heat transfer
$\Delta Q_j=U_j(T_{f,j}-T_{p,j})$

Interface temperatures
$T_{1,j}=\Delta Q_j/\alpha_{f,j}$, $T_{2,j}=\Delta Q_j/\alpha_{p,j}$

Flux
$J_j=C_{membrane,p}(P_{T1,j}-P_{T2,j})$

Overall heat transfer coefficient
$U_j=1/(1/\alpha_{p,j}+1/\alpha_{f,j}+1/(\lambda/b+J_jH_{latent}(T_{1,j}-T_{2,j}))$

Overall heat transfer
$\Delta Q_j=U_j(T_{f,j}-T_{p,j})$

Interface temperatures
$T_{1,j'}=T_{f,j}-\Delta Q_j/\alpha_{f,j}$, $T_{2,j'}=T_{p,j}-\Delta Q_j/\alpha_{p,j}$

No

Error = 0.5[Abs($T_{1,0}-T_{1,j'}$) / ($T_{1,j'}+T_{1,j}$) + Abs($T_{2,j'}-T_{2,j}$) / ($T_{2,j'}+T_{2,j}$)]< 10^{-8}

Yes

$T_{f,j+1}=T_{f,j}-\Delta Q_{j'}/(\dot{m}_{f,j}C_{p,f})$
$T_{p,j+1}=T_{p,j}-\Delta Q_{j'}/(\dot{m}_{p,j}C_{p,p})$

No

$T_{p,N}=T_{p,inlet}$

Fig. 2 Programming flow chart

3.2 Experiment

3.2.1 DCMD experiment

Experiments under different conditions were performed to assess the model predictions. A schematic diagram of the DCMD process is shown in Fig. 3. The detail for the experimental setup was given in [17], in which the flux from different conditions including six velocities (0.055 to 0.151 m/s or 300 to 800 mL/min), and five membrane lengths (5, 7, 9, 13 and 733 cm) were reported. The feed is 1 wt% NaCl solution. All flux results were measured over a period of 1.5 to 4 hours and variation in flux (calculated every half or one hour) over this time period was ±5%. Most experiments were repeated under the same conditions, and the variations of flux were also found to be in the range of ±5% when different membrane pieces from a bulky membrane roll were employed. Except for the data presented in Figure 7 showing the influence of membrane length on flux from different pieces of new membranes, all the data presented in each figure were from the same piece of membrane. Before the membranes were used, they were conditioned for 3 hrs at feed and permeate inlet temperatures of 60 and 20°C and velocity of 0.0945 m/s with the pressure control valves fully opened. In the conditioning period (no membrane compression), only the membranes with initial flux falling into the range of ±5% of the average flux were selected for further experiments.

The membrane used in these experiments was a PTFE membrane from Changqi with a mean pore diameter of 0.5 μm. The porosity of the membrane active layer was 92.5±0.5% measured by a wetting method [17]. The measured Liquid Entry Pressure (LEP) using the method provide in [16] was 80±5 kPa, the contact angle was 140±2.5° measured by the method described in [16] and the calculated tortuosity in [17] was 1.10 which is similar to available data [18, 19]. The channel was filled with a spacer as described in [14].
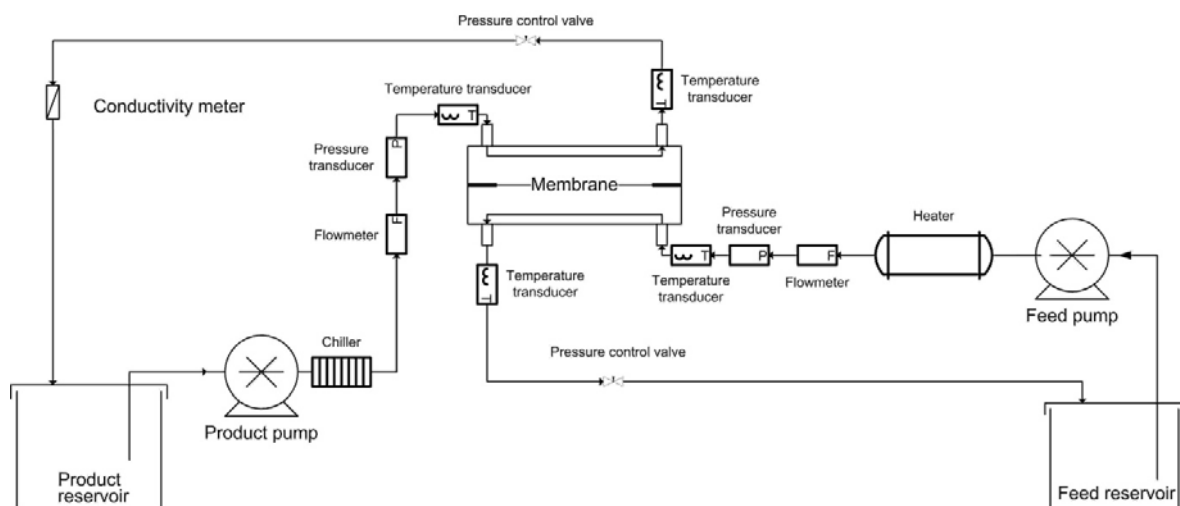

Fig. 3 Schematic of experimental process

3.2.2 Pressure drop experiment

The pressure drop across the module at different flowrates was measured experimentally with the DCMD module. The module channel was 0.8 mm high, 13 cm long (in the flow direction) and 13 cm wide (transverse to the flow direction). The feed and permeate streams at the identical velocities were controlled at inlet temperatures of 60 and 20°C. The pressure drops were measured at six different velocities (0.056 - 0.148 m/s or 300 - 800 ml/min) with

the pressure control valves fully open. The pressure drop after the outlets were neglected because the tube used was of large diameter (Ø = 15 mm) and short (< 50 cm), such that the pressure drop for the considered flows was negligible. The salt rejection in all tests was greater than 99.5% and was independent of the test pressures considered given they were all significantly below the LEP.

4. Results and Discussion

Fig. 4 shows the relationship between the pressure drop and the stream velocities, and an equation fitting the curve was extrapolated for calculation of the pressure drop in the modelling velocity range. The membrane compression was calculated using the pressure on the feed side (higher pressure side), according to the paper of Zhang et. al [17].

$$y = 248.36x^2 - 27.552x + 2.0084$$
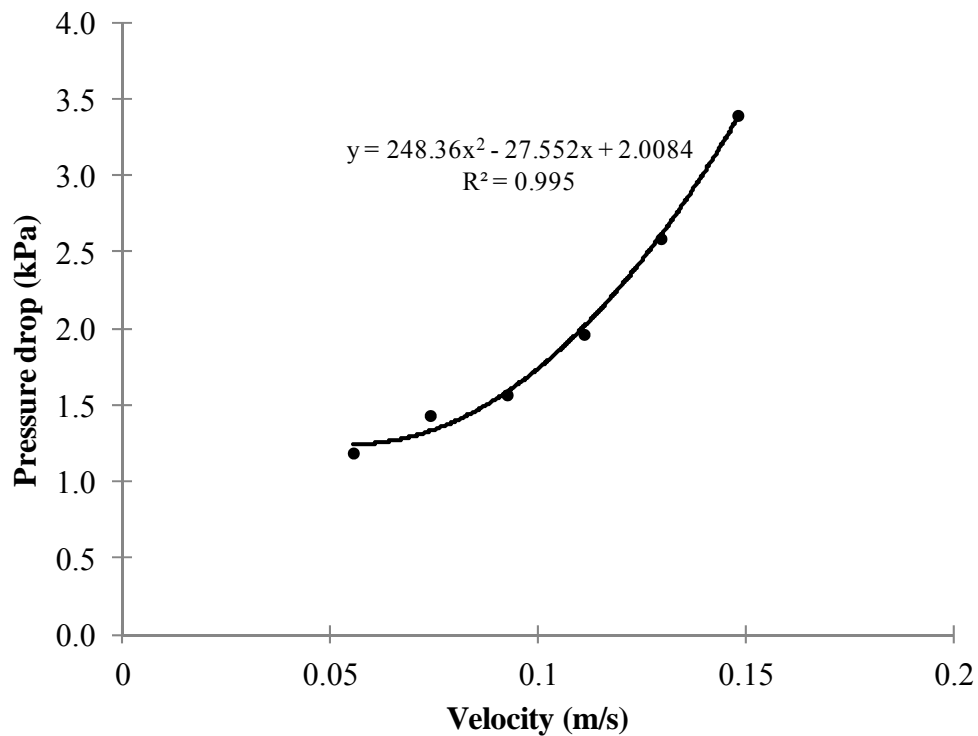$$R^2 = 0.995$$

Fig. 4 Pressure drops at different velocities

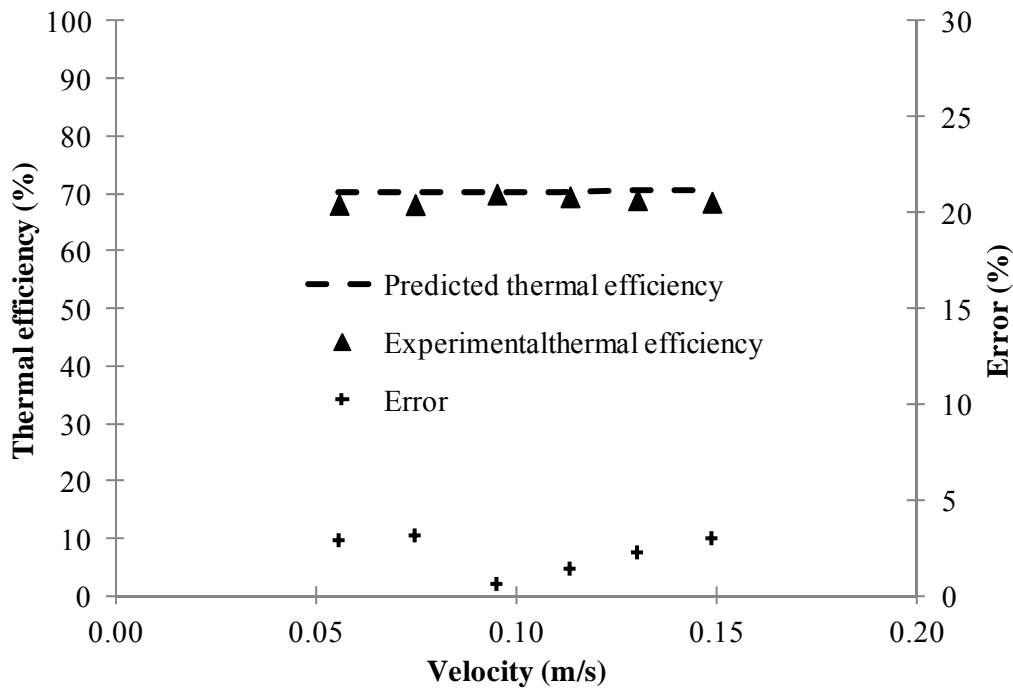4.1 Accuracy assessment of the model predictions

Fig. 5 Assessment of modelling program at different velocities

(Feed inlet temperature = 60°C, cold inlet temperature = 20°C, membrane length = 0.13 m,
Feed velocity = permeate velocity, ΔP < 2 kPa)

Fig. 5 shows the predicted and measured thermal efficiency at different feed velocities. Fig. 5 shows that the error between the predicted and the experimental results was within 5% and distributed randomly (the membrane was assumed incompressible, as the pressure was < 2 kPa). In comparison with the ±5% flux variation, the modelling error of thermal efficiency was similar and therefore acceptable. It was shown in previous research [3, 20, 21] that the DCMD flux will increase with increasing velocity due to enhanced heat transfer, which was also predicted by modelling results [14]. However, the thermal efficiency remains almost constant at different velocities. Therefore, if a low-grade heat source at a constant temperature is used for the feed stream, more thermal power will be required for the production of pure water at a higher velocity, because of the increased total mass and heat transfer. However, more pumping power (electricity) will also be consumed at high velocity. Thus, for an incompressible membrane, it is suggested to optimise the power consumption of pumping and the possible power extracted from the low grade heat source. If the increment of pumping power consumption (electricity) for increasing the stream velocity is greater than the energy gain from the low-grade heat source, it is sub-optimal to increase flux by using higher velocity.
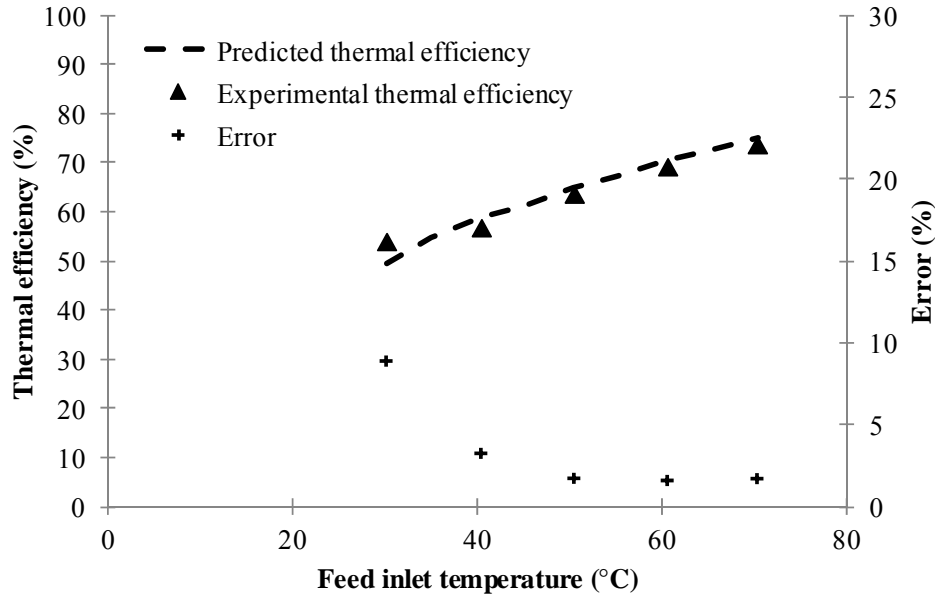
Fig. 6 Assessment of modelling program at temperatures
(Cold inlet temperature = 20°C, stream velocities = 0.113 m/s, membrane length = 0.13 m,
$\Delta P < 2$ kPa)

Fig. 6 shows the effect of different feed inlet temperatures on the thermal efficiency. Most of the errors were less than 4%, except for a feed inlet temperature of 30°C (8.9%) which was outside the range of ±5% experimental variation. The errors decreased and flattened out at higher temperatures (50 - 60°C). Since the predicted thermal efficiency is higher than the experimental results, theoretically the error should become greater than that of the lower temperature due to higher temperature and concentration polarisation effects [16, 22].

Therefore, it was considered that this largest error may be due to inaccuracy in measuring the temperature, which was not directly related to the measured flux. Mass flowrates are decreasing on the feed side and increasing on the permeate side due to mass transfer across the membrane. Therefore, based on Eq. (4), the temperature difference between inlet and outlet on the feed side (ΔT_f) should be greater than that of on the permeate side (ΔT_p).

$$\dot{m}_f \Delta T_f C_{p,f} = \dot{m}_p \Delta T_p C_{p,p} \tag{4}$$

where $\dot{m}_f$ and $\dot{m}_p$ are respective mass flowrates on feed and permeate sides, and $C_{p,f}$ and $C_{p,p}$ are the specific heats on feed and permeate sides, which have negligible variation with temperatures (C_p = 4.1818 J·g⁻¹K⁻¹ at 20°C and C_p = 4.1843 J·g⁻¹K⁻¹ at 60°C [23]). Hence, at higher temperature, the difference between ΔT_f and ΔT_p should become greater due to the higher flux. Although this trend was predicted by the model (0.01 and 0.34°C respectively at 30 and 70°C), this phenomena was not observed experimentally (both 0.4°C at 30 and 70°C). If the temperature difference of 0.4°C at 30°C was ignored, the prediction error will be 4.5%, which is within the experimental variation range.

From Fig. 6, it also can be found that the thermal efficiency increased almost linearly with temperature, although the flux was found to increase exponentially with temperature from the previous works [3, 20, 21, 24]. Therefore, it is suggested to make the feed inlet temperature as high as possible, which will benefit both the thermal efficiency and the flux. For example, if a solar panel was used as a heat source, it is important to control the stream velocity of the heating medium so as to acquire a high temperature.
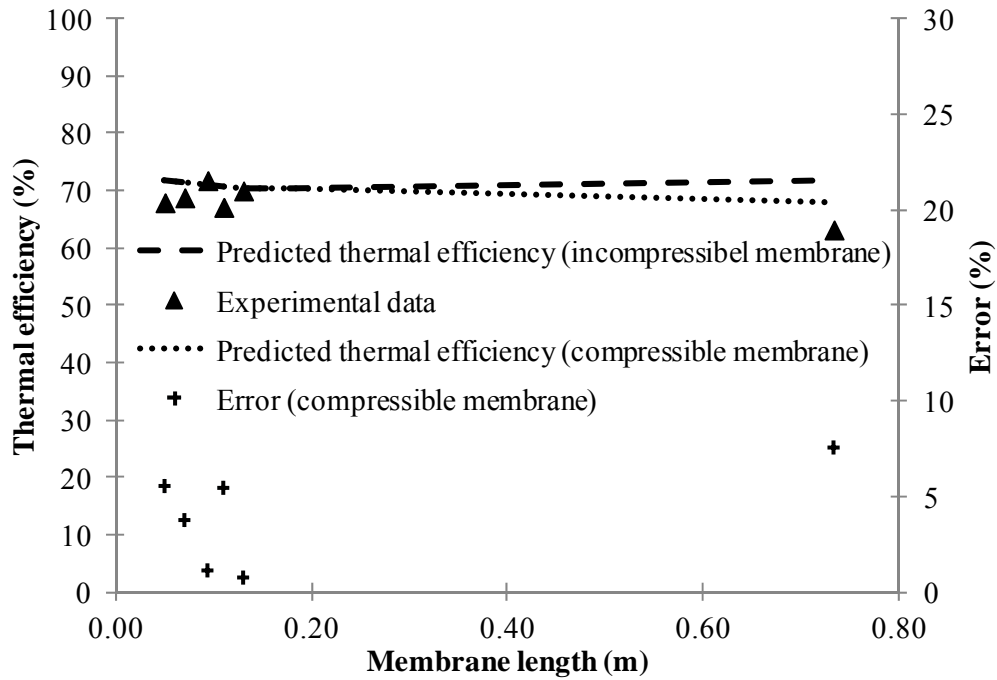
Fig. 7 Assessment of modelling program with different membrane lengths
(Feed inlet temperature = 60°C, cold inlet temperature = 20°C, stream velocities = 0.113 m/s)

The model predictions for variations in membrane length are shown in Fig. 7. The differences (error within 5.5%) between the predicted and measured thermal efficiency is relatively small when the membranes are short, regardless of whether or not the membrane is compressible or incompressible. However, when a 0.733 meter membrane is employed, the error of the predicted result based on the incompressible membrane is over 13%, but error of predicted result based on a compressible membrane is about 7.5%. When the membrane length was short, the pressure drop along the membrane was negligible (0 - 2 kPa) and the effect of compression is small. However, the effect of compression was noticeable for the 0.733 meter membrane as the pressure drop increased to 13 kPa due to the much longer flowing channel. From Fig. 7, it also can be found that the thermal efficiency of the incompressible membrane will be independent of the membrane length, while the thermal efficiency for compressible membranes was predicted to decline as the membrane becomes longer. It can be speculated from Eq. (2) that the compressible membrane, unlike the incompressible membrane, will become thinner and less porous when higher pressure is applied on its surface. According to the calculation in Eq. (2), the membrane thermal conductivity of the compressible membrane will increase, so as to result in more sensible heat loss. Because the feed inlet temperature and velocity is the same, the increased sensible heat loss will reduce the energy used for evaporation and cause a reduction in thermal efficiency (Eq. (3)).

Flux decline for both incompressible and compressible membranes were observed in previous works [4, 14], and thermal efficiency decline was found in this study as the membrane became longer. Therefore, it is not recommended to use very long membranes (in flowing direction), because it will increase the pumping energy consumption (greater resistance) and reduce the flux [4, 14], even if an incompressible membrane is employed.

4.2 Predicting influence of process parameter on the thermal efficiency

Based on the preceding assessment it appears that for the PTFE membrane considered in this work, it can be assumed to be incompressible when the membrane length is short and the stream velocities low (0.15m/s).
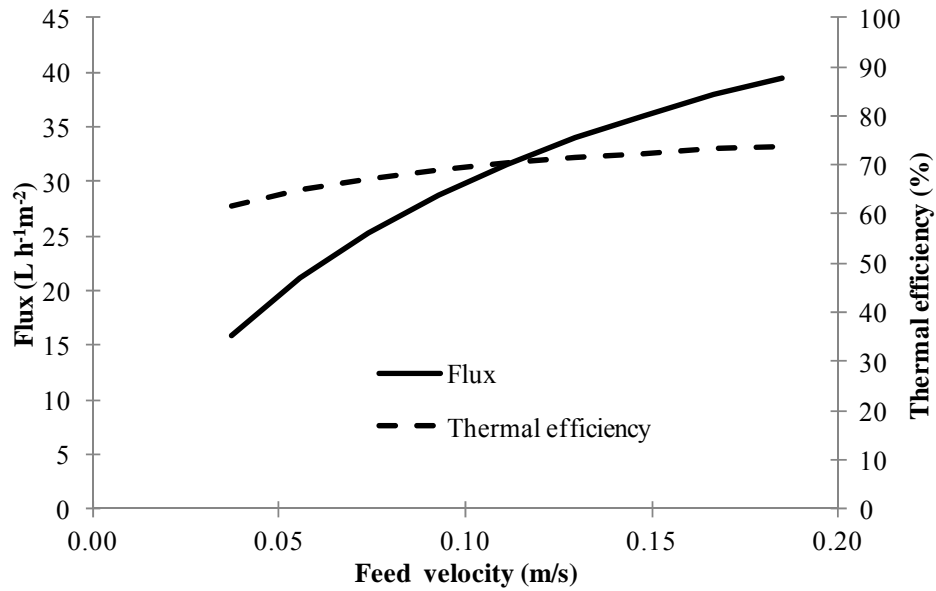
a. Predicted flux and thermal efficiency at different feed velocities for incompressible membrane
(Feed inlet temperature = 60°C, cold inlet temperature = 20°C, permeate velocity = 0.113 m/s, membrane length = 0.13 m)
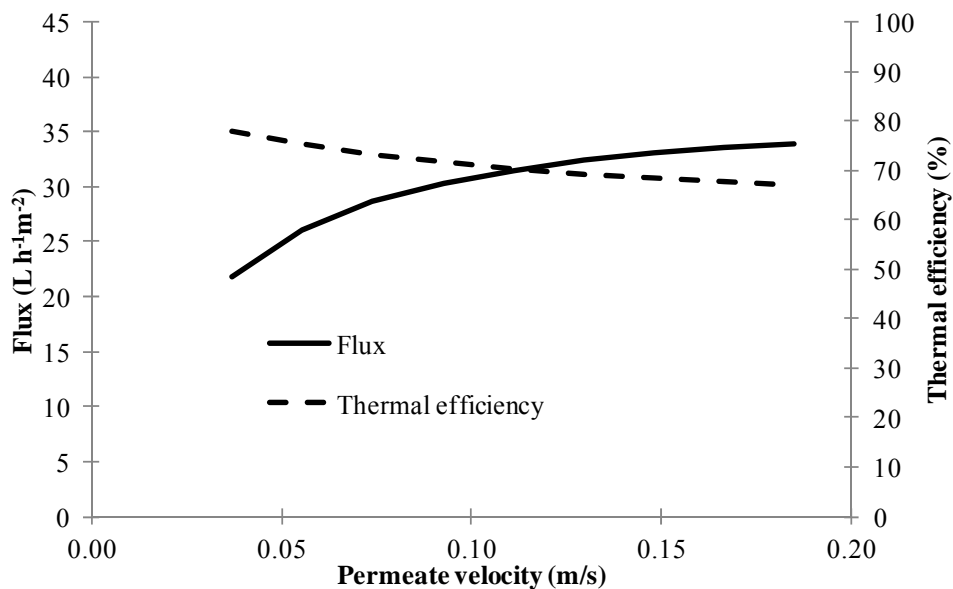
b. Predicted flux and thermal efficiency at different permeate velocities for incompressible membrane
(Feed inlet temperature = 60°C, cold inlet temperature = 20°C, feed velocity = 0.113 m/s, membrane length = 0.13 m)

Fig. 8 Influence of velocity on thermal efficiency and flux

In Figs. 8a and 8b, the dependency of flux and thermal efficiency on stream velocities is predicted for an incompressible membrane, in which the stream velocity was varied on one side of the membrane and fixed on the other side of the membrane. Since the increased velocity will make the flow more turbulent which will enhance the heat transfer from the bulk of the feed stream towards the membrane, and the heat transfer from the fluid near the membranes surface to the bulk in the permeate stream, increasing the velocity on either side of the membrane will produce more flux as predicted in Figs. 8a and 8b. Additionally, with the same increase in magnitude, increasing the feed velocity will produce more flux than that of increasing permeate velocity. However, increasing velocity on different sides of the membrane has counter influence on the thermal efficiency. In Fig. 8a, the thermal efficiency increases with the increasing feed velocity, but decreases with the increasing velocity of the permeate stream (see Fig 8b).

This reverse tendency is caused by the interface temperature changes under the two different conditions. If the permeate velocity is kept constant while the feed velocity increases, the mean interface temperature on the feed side (T_1) will increase due to the increased turbulence. However, if the feed velocity is kept constant, an increased permeate velocity will cause a decrease of the mean T_1, due to the increased sensible heat loss caused by the reduced mean interface temperature on the permeate side (T_2). As the feed and permeate velocities increased from A to B as shown in Figs. 8a and 8b, it can be assumed the mean feed and permeate interface temperatures are changed by the same amplitude. However, the feed interface temperature change will cause more vapour pressure change than that of the permeate due to the exponential relationship between the temperature and vapour pressure. For example, assuming initial feed and permeate interface temperatures are 50 and 30°C respectively, as the velocity on one side increases, the temperature difference rises from 20 to 20.1°C. If the 0.1°C difference incurred by increasing feed velocity (interface temperature rises from 50 to 50.1°C), the increase in vapour pressure difference across the membrane is 61.4 Pa. However, if it was incurred by increasing permeate velocity (interface temperature reduces from 30 to 29.9°C), the increase in vapour pressure difference is 24.3 Pa. The sensible heat loss through the membrane is equal in both cases, but there is more latent heat loss from increasing feed velocity than increasing permeate velocity.
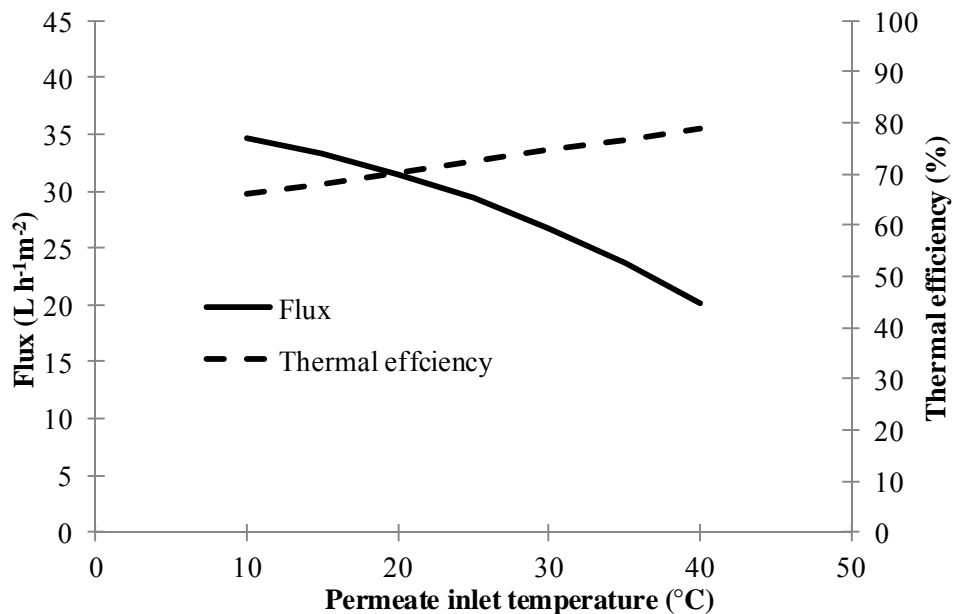
Fig. 9 Influence of permeate inlet temperature on thermal efficiency and flux for incompressible membrane
(Feed inlet temperature = 60°C, membrane length = 0.13 m, stream velocities = 0.113 m/s)

Fig. 9 shows the influence of increasing permeate temperature on thermal efficiency and flux. The large decrease of flux was found as the permeate inlet temperature increased. However, the thermal efficiency of the process shows increase with temperature.

Table 1. Vapour pressure and sensible heat loss changed with increasing permeate interface temperature (Assuming the initial feed and permeate interface temperatures 60 and 20°C)

Permeate interface temperature	30°C	40°C	50°C
Sensible heat loss reduction (%)	25.0	50.0	75.0
Vapour pressure reduction (%)	10.8	28.7	56.9

From Table 1, it can be found that the sensible heat reduction is greater than the vapour pressure reduction as the permeate interface temperature increases. The latent heat loss is linear to the vapour pressure and based on Eq. (3), an increase of thermal efficiency will be achieved as the permeate inlet temperature rises.
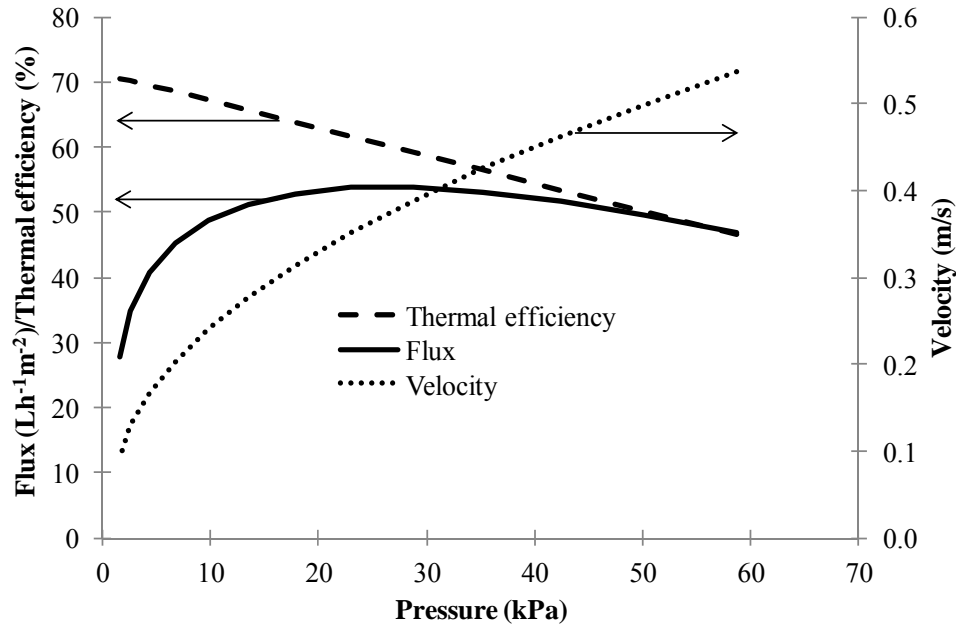

Fig. 10 Influence of stream velocities on thermal efficiency and flux for compressible PTFE membranes
(Feed inlet temperature = 60°C, cold inlet temperature = 20°C, membrane length = 0.13 m, same stream velocities)

The effect of membrane compression will become significant for long membranes and fast stream velocities, as the pressure increases with these changes in operating conditions. The effect of membrane length on compressible PTFE membranes was shown in Fig. 7, while Fig. 10 shows the predicted thermal efficiency and flux affected by simultaneously increasing stream velocities for compressible PTFE membranes. In Fig. 5, the presented velocity (0 - 0.17 m/s) is in the capacity range (0 - 900 mL/min) of the peristaltic pump employed in the

experiment, for which the pressure drop on the membrane was negligible (0 - 3 kPa) as shown in Fig. 4.

The relationship between the pressure and the stream velocity presented in Fig. 4 and the compressibility of the membrane under static pressure shown in [14, 17] was used in the modelling program. The module had very low hydraulic resistance, so to achieve a greater pressure drop (35 kPa at 0.42 m/s) and compress the membrane required velocities much higher than the experimental pump capacity. The flux approaches a plateau with increasing velocity [16], but the hydraulic pressure increases via a square relationship to the velocity. Therefore, the flux increases initially with rising velocity at low velocities where the pressure is low and increases in turbulence are significant. However, at higher velocities where the pressure is high and turbulence is not the controlling factor for flux, the flux decreases as the velocity increases. From Fig. 5, it can be found that the thermal efficiency is not affected by simultaneously increasing stream velocities if an incompressible membrane is used because the thermal conductivity will not change. Therefore, it can be speculated that the thermal efficiency will decrease if a compressible membrane is used, because the thermal conductivity becomes greater at the higher velocity which incurs a greater pressure drop on the membrane surface. The predicted flux increased initially with the escalating velocity, reached a peak at a velocity of 0.39 m/s (pressure ≈ 30 kPa, calculated from equation in Fig. 4), and decreased for velocities above 0.4 m/s, which is different from that of incompressible membranes [3, 20, 21]. For compressible membranes, the thermal efficiency decreased as the velocity increased, which is also different from the results shown in Fig. 5, and the relationship between the thermal efficiency and static pressure was discussed in paper [14]. Therefore, it is suggested to choose the stream velocity carefully if a compressible membrane is used, because increasing the velocity can reduce both the flux and thermal efficiency for DCMD in a manner similar to increasing the backpressure on the system. Incompressible membranes may have an advantage for DCMD under conditions of high channel pressure.

5. Conclusions

A mathematical model capable of predicting the thermal efficiency and flux for DCMD processes using a compressible membrane was developed based on mass and heat transfer balances and the assumption of unchanged tortuosity with membrane compression [14].

The model predictions were compared with experimental results at different temperatures, velocities, membrane lengths and pressures. Except for the result with feed temperature at 30°C, most of the errors were within ±5% which is within the experimental variation range. Experiments for long modules and high velocities could not be conducted experimentally, but the model was extrapolated to this region to predict DCMD performance.

From the model predictions, it is suggested that:
- Employing high feed velocity in the DCMD process will obtain both high flux and high thermal efficiency for an incompressible membrane, but was predicted to lead to lower thermal efficiency and even cause flux decline for compressible membranes once the membrane begins to compress (>20kPa for PTFE membranes).
- In the case that the thermal energy will be recovered from the permeate side, using long incompressible membranes (but it is also limited by LEP) will achieve a high permeate outlet temperature and will not alter the thermal efficiency.
- The thermal efficiency is independent of simultaneous increases of feed and permeates stream velocities for incompressible membranes, although the flux increases. If only the feed velocity is increased, both the flux and thermal

efficiency are increased. Increasing the cold stream velocity also increases the flux but the thermal efficiency decreases.

- Both the predicted and experimental results show that high-temperature feed will improve DCMD energy efficiency and productivity compared to operation at low feed temperatures. Although raising the cold stream inlet temperature will result in a dramatic decrease of flux, it also leads to an increase of the thermal efficiency.
- In a scaling up DCMD using compressible PTFE membranes, it is necessary to reduce the pressure drop along the module, e.g., reduce the membrane length in the flow direction and the flow velocities. Therefore, increasing the membrane width (transverse to the stream flows) rather than the length in the flow direction will maintain high flux in scaling up designs, which will maintain both high flux and thermal efficiency. To improve the flow distribution as the module becomes wider, multiple inlets in the width direction can be used [25].
- Since the operating temperature is normally not adjustable when low grade waste heat is employed, optimising the flowrates and pressure drops for compressible membranes are the key factors for optimising flux and thermal efficiency for large modules.

Acknowledgments

Nomenclature

α_f, α_p	heat transfer coefficient on feed side and permeate side
A	membrane area
b	membrane thickness
C_0	membrane mass transfer coefficient
C_{pp}, C_{pf}	specific heat of water on permeate and feed sides
d	mean pore diameter of the membrane
d_f	filament diameter
d_h	hydraulic diameter
D_{AB}	the diffusivity of water vapour (A) relative to air (B)
ε	membrane porosity
g	acceleration due to gravity
h_{latent}	latent heat of water vaporisation
J	vapour flux through the membrane
J_m, J_k	vapour flux through membrane pore arising from molecular and Knudsen diffusion
κ	thermal conductivity of the water
Kn	Knudsen number
l	mean molecular free path

λ	thermal conductivity of membrane material
λ_{air}	thermal conductivity of air
λ_m	thermal conductivity of membrane
$\dot{m}_f, \dot{m}_p$	mass velocity on the feed and permeate sides
m_{total} and $m_{support}$	the masses of the membrane with the support layer and the support layer
M	the molecular weight of water
Nu	Nusselt number
P	total pressure in the pore
P_A	partial vapour pressure in the pore
P_r	Prandtl number
P_{T1}, P_{T2}	vapour pressure at T_1 and T_2
ρ	water density
ρ_{PTFE}	PTFE density
Q	overall heat transfer
R	universal gas constant
Re	Reynolds number
τ	pore tortuosity
T	mean temperature in the pore
T_f, T_p	bulk temperatures of feed and permeate
$T_{fi}, T_{fo}, T_{pi}, T_{po}$	inlet and outlet temperatures of feed and permeate
T_1, T_2	feed and permeate temperatures at liquid-vapour interface
TPC	temperature polarisation coefficient
μ	water viscosity
V	volume of active layer
$V_{filament}, V_{total}$	filament and total volumes of spacer
x	distance from feed inlet
x_A	mole fraction of water vapour in the pore
W	membrane width

References

[1] F. Banat, R. Jumah, M. Garaibeh, Exploitation of solar energy collected by solar stills for desalination by membrane distillation, Renewable Energy. 25 (2002) 293-305.

[2] P. K. Weyl, Recovery of demineralized water from saline waters, U. S. A, (1967).

[3] K. W. Lawson, D. R. Lloyd, Membrane distillation, Journal of Membrane Science. 124 (1997) 1-25.

[4] Z. Lei, B. Chen, Z. Ding, Membrane distillation, in: Z. Lei, B. Chen, Z. Ding (Eds.), Special Distillation Processes, Elsevier Science, Amsterdam, 2005, pp. 241-319.

[5] W. T. Hanbury, T. Hodgkiess, Membrane distillation - an assessment, Desalination. 56 (1985) 287-297.

[6] R. W. Schofield, A. G. Fane, C. J. D. Fell, Heat and mass transfer in membrane distillation, Journal of Membrane Science. 33 (1987) 299-313.

[7] L. Carlsson, The new generation in sea water desalination SU membrane distillation system, Desalination. 45 (1983) 221-222.

[8] K. Schneider, T. J. van Gassel, Membrandestillation, Chemie Ingenieur Technik. 56 (1984) 514-521.

[9] S. I. Andersson, N. Kjellander, B. Rodesjö, Design and field tests of a new membrane distillation desalination process, Desalination. 56 (1985) 345-354.

[10] F. Edwie, M. M. Teoh, T.-S. Chung, Effects of additives on dual-layer hydrophobic–hydrophilic PVDF hollow fiber membranes for membrane distillation and continuous performance, Chemical Engineering Science. 68 (2012) 567-578.

[11] S. Bonyadi, T. S. Chung, Flux enhancement in membrane distillation by fabrication of dual layer hydrophilic-hydrophobic hollow fiber membranes, Journal of Membrane Science. 306 (2007) 134-146.

[12] P. Wang, M. M. Teoh, T.-S. Chung, Morphological architecture of dual-layer hollow fiber for membrane distillation with higher desalination performance, Water Research. 45 (2011) 5489-5500.

[13] J. A. Prince, G. Singh, D. Rana, T. Matsuura, V. Anbharasi, T. S. Shanmugasundaram, Preparation and characterization of highly hydrophobic poly(vinylidene fluoride) – Clay nanocomposite nanofiber membranes (PVDF–clay NNMs) for desalination using direct contact membrane distillation, Journal of Membrane Science. 397–398 (2012) 80-86.

[14] J. Zhang, S. Gray, J.-D. Li, Modelling heat and mass transfers in DCMD using compressible membranes, Journal of Membrane Science. 387–388 (2012) 7-16.

[15] V. A. Bui, L. T. T. Vu, M. H. Nguyen, Simulation and optimisation of direct contact membrane distillation for energy efficiency, Desalination. 259 (2010) 29-37.

[16] J. Zhang, N. Dow, M. Duke, E. Ostarcevic, J.-D. Li, S. Gray, Identification of material and physical features of membrane distillation membranes for high performance desalination, Journal of Membrane Science. 349 (2010) 295-303.

[17] J. Zhang, J.-D. Li, S. Gray, Effect of applied pressure on performance of PTFE membrane in DCMD, Journal of Membrane Science. 369 (2011) 514-525.

[18] R. W. Schofield, A. G. Fane, C. J. D. Fell, Gas and vapour transport through microporous membranes. II. Membrane distillation, Journal of Membrane Science. 53 (1990) 173-185.

[19] C.-C. Ho, A. L. Zydney, Measurement of membrane pore interconnectivity, Journal of Membrane Science. 170 (2000) 101-112.

[20] E. Curcio, E. Drioli, Membrane Distillation and Related Operations: A Review, Separation and Purification Reviews. 34 (2005) 35 - 86.

[21] L. Martínez, J. M. Rodríguez-Maroto, Effects of membrane and module design improvements on flux in direct contact membrane distillation, Desalination. 205 (2007) 97-103.

[22] V. A. Bui, L. T. T. Vu, M. H. Nguyen, Modelling the simultaneous heat and mass transfer of direct contact membrane distillation in hollow fibre modules, Journal of Membrane Science. 353 (2010) 85-93.

[23] Y. A. Cengel, M. A. Boles, Thermodynamics: an engineering approach. 6th ed., McGraw-Hill, New York, 2008.

[24] F. A. Banat, J. Simandl, Desalination by Membrane Distillation: A Parametric Study, Separation Science and Technology. 33 (1998) 201-226.

[25] N. Dow, S. Gray, J.-d. Li, J. Zhang, E. Ostarcevic, A. Liubinas, P. Atherton, D. Halliwell, M. Duke. Power station water recycling using membrane distillation - A plant trial. in Ozwater. 2012. Sydney.